Journal of Thermal Analysis and Calorimetry (2022) 147:5473–5481
https://doi.org/10.1007/s10973-021-11176-5

Thermo-mechanical properties and electrical mapping of nanoscale domains of carbon-based structural resins

Marialuigia Raimondo[1] · Carlo Naddeo[1] · Michelina Catauro[2] · Liberata Guadagno[1]

Received: 12 June 2021 / Accepted: 4 December 2021 / Published online: 4 January 2022

Abstract
Carbon nanostructured forms, such as one-dimensional (1D) carbon nanofibers (CNFs) and two-dimensional (2D) graphene nanoplatelets (GNPs), are increasingly attracting the attention of scientists whose studies are aimed at obtaining superior nanocomposites with unrivaled performance and/or unprecedented properties. In this work, nanocomposites loaded with different mass percentages of carbonaceous nanoparticles (CNFs, GNPs) capable to exhibit discrete electrical conductivity have been investigated using differential scanning calorimetry (DSC), dynamic mechanical analysis (DMA), and tunneling atomic force microscopy (TUNA). DSC and DMA investigations highlighted that an appropriate chemical composition of the hosting matrix, together with a suitable two-stage curing cycle allows formulating structural resins characterized by high values of the curing degree (higher than 97%), glass transition temperature (also higher than 250 °C), and storage modulus (higher than 3000 MPa at room temperature). TUNA analysis evidences a satisfactory distribution of the conductive nanofiller on nanometric domains.

Keywords Thermosetting resins · Carbonaceous nanofillers · Thermal analysis · Mechanical properties · Tunneling atomic force microscopy (TUNA)

Introduction

Carbon nanomaterials, such as one-dimensional CNFs and two-dimensional GNPs, exhibit an extensive variety of singular thermal, mechanical, and electrical properties that make them ideal candidates for their use as additives in the preparation of multifunctional polymeric composites, thus opening a way toward new applications in the fields of materials science and technology [1–6]. In particular, they are able to contrast the photooxidative degradation of polymeric systems [7, 8]. Furthermore, carbon nanostructured forms are very useful because they can be employed to improve many properties of polymeric systems to which they also confer functional properties [9–13]. It is well known that in the polymer field, epoxy resins are one of the most frequently used polymer matrices for advanced composite applications [14–17] as they possess good stiffness and specific strength, dimensional stability, chemical resistance, and also strong adhesion to the enclosed reinforcement [18]. The preparation of epoxy resins reinforced with CNFs and GNPs needs a homogeneous dispersion and a strong interfacial interaction between the carbon nanofiller and the polymer. The addition of a reactive diluent 1–4 butanedioldiglycidyl ether (BDE) to a thermoset resin, such as tetraglycidylmethylenedianiline (TGMDA), has proven its effectiveness in reducing resin viscosity [19] in processing, thus improving the processability and simultaneously determining a better nanofiller distribution. Viscosity reduction is markedly auspicious for epoxy resins loaded with nanofillers which have a tendency to drastically growth the resin viscosity, which represents a very limiting criticality from a processing point of view. A targeted composite material design is of utmost importance if we consider their use for a real industrial application, such as the fuselage reinforcement on commercial aircraft. In this work, the choice of using 4,4′-diaminodiphenylsulfone (DDS) as curing agent together with the BDE diluent and the TGMDA epoxy precursor allowed to obtain a matrix formulation suitable for the production of composites with exceptional properties

✉ Marialuigia Raimondo
mraimondo@unisa.it

[1] Department of Industrial Engineering, University of Salerno, Via Giovanni Paolo II, 132, 84084 Fisciano, Italy

[2] Department of Engineering, University of Campania "Luigi Vanvitelli", via Roma 29, 81031 Aversa,, Italy

that guarantee their use in the aeronautical and space sector. The materials utilized in aeronautical vehicles are normally exposed to severe aerodynamic loads, thermal and oxidative environments, which lead to fast, continuous overlapping degradation mechanisms. The primary structures for these vehicles need to be lightweight, very strong, and rigid to preserve mechanical properties during service conditions [20, 21]. One of the key properties of nanocomposites includes functioning at elevated and sub-zero temperatures, which made them adapted for the extreme conditions of outer space and the lower earth orbit [22]. Besides, an aircraft fuselage needs to be made of conductive material to guarantee that lightning strikes can have a steady flow, without damaging the internal structure of the aircraft. In this contest, thermomechanical analysis that investigates how material properties vary with temperature plays a major role. Because of this, carbon nanostructured forms, such as carbon nanofibers (CNFs) and graphene nanoplatelets (GNPs), are the leading candidates for such aeronautical applications requiring materials characterized by high curing degree and highly cross-linked structure with strong interconnections between the conductive nanoparticles and the host matrix. The nanoparticles CNFs and GNPs have excellent mechanical properties, high thermal and electrical conductivities, which can be effectively transferred to the host thermosetting matrix, thus giving rise to advanced composites with the ability to withstand high temperatures. The mechanical, electrical, and thermal properties of composites are strongly dependent on their material composition, method of fabrication, and constituent percentages. In particular, the thermal behavior of carbon nanomaterials and their corresponding nanocomposites is crucial to determine their fields of application [23].

The purpose of this paper is to formulate both carbon nanofibers (CNFs)/epoxy resins and graphene nanoplatelets (GNPs)/epoxy resins using the same matrix formulation and the same two-stage curing cycle, following a sonication as a tool to effectively disperse the carbon nanoparticles, and to investigate the thermal, mechanical, and electrical properties by TUNA of the resulting nanocomposites. In this work, we found that carbon nanofibers (CNFs) and graphene nanoplatelets (GNPs) are both effective as nanoscale reinforcement for the chosen epoxy formulation, thus demonstrating their ability to impart multifunctional properties to the epoxy matrix in which they are homogeneously dispersed. In particular, in the present study, polymer composites with mass fractions of CNFs ranging from 0.05–2 mass% and mass fractions of GNPs ranging from 0.025–1.8 mass% are formulated. The curing degree evaluation of the nanofilled epoxy samples was achieved by DSC thermal analysis. The effect of both 1D and 2D nanofillers on the mechanical behavior of the final composites was instead investigated by DMA. The remarkable mechanical properties surely connected to the elevated curing degree (around 100% for CNF/epoxy resins and higher than 90% for GNP/epoxy resins) obtained with the selected formulation and curing process, together with the notable electrical current values at nanoscale level recorded for the investigated nanocomposites and the good nanocharge distribution and interactions at the nanoscale (by TUNA tool), put emphasis on the real potentiality offered by CNFs and GNPs in paving the way for the multifunctional materials suitable for application in various industrial sectors where also functional properties are required.

Experimental

Materials

The carbon nanofibers (CNFs) used in this work belong to the Pyrograf III family and appear in a free-flowing powder form. (Typically 99% mass is in a fibrous form.) They were heat-treated at 2500 °C in order to obtain an effective compromise between electrical and mechanical properties [5]. For the CNFs, the density is between 1.4 and 1.6 g cm^{-3}, the specific surface area is 54 m^2 g^{-1}, the average pore volume is 0.120 cm^3 g^{-1}, and the average pore diameter is 89.30 angstroms. CNFs are characterized by very straight and smooth walls due to the heat treatment they have undergone, as it can be easily seen from the FESEM image of the carbon nanofibers in Fig. 1. The graphene nanoplatelets (GNPs) are characterized by 60% of degree of amorphous phase (AP) [24]. They were prepared by treating natural graphite, whose average diameter is 500 μm, with a nitric and sulfuric acid mixture. After a day of reaction, the graphite intercalated compound (GIC) formed was subjected to an instantaneous thermal treatment of 900 °C, and quick expansion then has occurred. The percentage of carboxylated groups on the GNPs edges was found to be 10 mass%, and the number of stacked monolayer sheets is 29 [24], taking as a reference the thickness of a single graphene layer which is approximately 0.34 nm [25]. An average thickness of about 0.980 Å was detected. Figure 2 shows the FESEM picture of the GNPs, where overlapped graphene sheets are clearly visible.

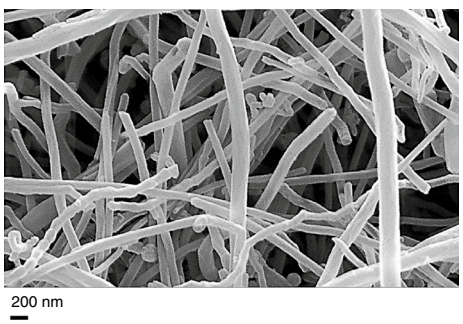

Fig. 1 FESEM image of CNFs

The unfilled epoxy resin (ER) was done by blending TGMDA (80 mass%) with BDE (20 mass%) at which the curing agent DDS was inserted in stoichiometric amount. All these products were bought from Sigma-Aldrich. The epoxy blend and the DDS were mixed at 120 °C; the carbon nanofibers CNFs and graphene nanoplatelets GNPs were, then, added and homogeneously dispersed into the matrix by ultrasonication for 20 min to obtain the respective nanocomposites. In particular, in this study, within the unfilled epoxy resin (ER) the CNFs were dispersed at the 0.05, 0.32, 0.64, 0.8, 1, 1.3, and 2 mass% content and the GNPs at the 0.025, 0.1, 0.32, 0.5, 1, and 1.8 mass%. The CNFs- and GNPs-based nanocomposites are labeled ER + X%CNFs and ER + X%GNPs, respectively, where X% expresses the different mass% of CNFs and GNPs. It is worth noting that percentages up to 1.3 mass% allow a homogeneous dispersion of the carbon nanofibers in the epoxy matrix, while percentages over 1.3 mass% cause a growth in viscosity [26]. Besides, for the epoxy samples filled with CNFs, the electrical percolation threshold (EPT) lies in the confined interval between 0.05 and 0.32 mass% [5], while for those filled with GNPs, the EPT is in the range from 0.025 to 0.1 mass%. Hence, in correspondence with low GNPs loading percentages, high electrical conductivity values were recorded. Such values have never been observed at such a low EPTs for systems loaded with 2D fillers. These low EPTs are instead detected for 1D carbon nanofillers, namely carbon nanotubes (CNTs) or carbon nanofibers (CNFs) [19]. All the epoxy mixtures were solidified at 125 °C for 1 h and then at 200 °C for 3 h.

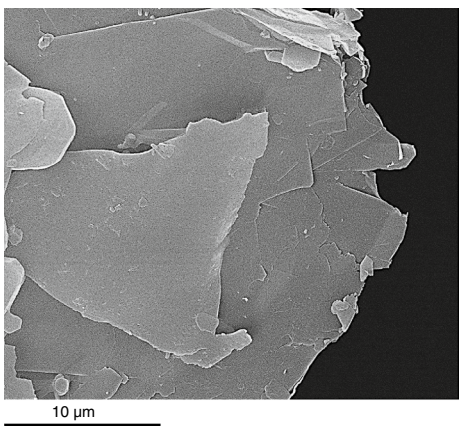

Fig. 2 FESEM image of GNPs

Methods

Morphological images of the CNFs and GNPs carbon nanofillers were captured using a field emission scanning electron microscope—FESEM (mod. LEO 1525, Carl Zeiss SMT AG, Oberkochen, Germany)—at a working distance of 4–8 mm with an acceleration voltage of 3.0 kV.

The DSC thermal characterization of both the unfilled epoxy resin (ER) and the two types of samples ER + X%CNFs and ER + X%GNPs, based on the 1D and 2D carbon nanoparticles at different loading percentages, was carried out by a Mettler DSC 822/400 instrument (Mettler-Toledo Columbus, OH, USA) in a flowing nitrogen atmosphere.

The cured samples were investigated between 0 °C and 300 °C at 10 °C min^{-1}. For reactions accomplished in isothermal conditions, the degree of curing (DC), which describes the conversion achieved during cross-linking reactions (curing) that generate a three-dimensional network, is most worthwhile for characterizing the sample properties. It can be defined by executing a series of isothermal experiments at different temperatures. More precisely, by means of the DSC data, it was possible to calculate the degree of curing (DC) of the samples, as shown below:

$$DC = \frac{\Delta H_{\mathrm{iso}}(T)}{\Delta H_{\mathrm{TOT}}} \times 100 \quad (1)$$

where $\Delta H_{\mathrm{iso}}(T)$ is the total heat of curing reaction at temperature T and ΔH_{TOT} is the total heat released during reaction.

A dynamic mechanical thermo-analyzer (Tritec 2000 DMA-Triton Technology) [5] was used to evaluate the mechanical performance of the samples. A variable flexural deformation in three points bending mode was applied. The mechanical tests were carried out in a temperature range between − 90 °C and 310 °C at the scanning rate of 3 °C min^{-2}, frequency of 1 Hz, and displacement amplitude of 0.03 mm.

The electrical mapping of nanoscale domains of carbon-based samples was done by TUNA (Veeco Instruments Inc.). Here, we show the TUNA images of the nanocomposites ER + 1.3%CNFs and ER + 1.8%GNPs containing percentages of nanofillers (i.e., 1.3 mass% of CNFs and 1.8 mass% of GNPs) above the EPT for which the highest conductivity values of 1.37 S/m and 0.096 S/m were measured, respectively. In order to better distinguish the morphological features of the carbon nanofibers and graphene nanoplatelets, the slices of the aforementioned filled resins, before being analyzed, were treated with an etching solution described in detail in previous papers [2, 4, 5]. The TUNA acquisitions were carried out in contact mode, appropriately setting the control parameters [5].

Results and discussion

In this work, the degree of curing (DC) has been evaluated in dynamic and isothermal regime. It is worth noting that the choice to consider the isothermal regime is dictated by the fact that several processes in the industry are really realized isothermally. The degree of curing (DC) attained in dynamic regime has been compared with the degree of curing (DC) of the epoxy samples after a programmed curing cycle of 125 °C for 1 h and then 200 °C for 3 h, carried out in an oven under isothermal conditions. DSC curves of the unfilled epoxy resin (ER) and epoxy resins filled with different CNF mass loading percentages cured under dynamic (Fig. 3) and isothermal (Fig. 4) heating conditions together with the percent values of the degree of cure (DC) of the epoxy resins filled with different CNF mass loading percentages cured under dynamic and isothermal heating conditions (Fig. 5) are shown. Moreover, DSC curves of the unfilled epoxy resin (ER) and epoxy resins filled with different GNP mass loading percentages cured under dynamic (Fig. 6) and isothermal (Fig. 7) heating conditions together with the percent values of the degree of curing (DC) of the epoxy resins filled with different GNP mass loading percentages cured under dynamic and isothermal heating conditions (Fig. 8) are also shown. In particular, in the dynamic regime, the uncured ER resin and nanocomposites loaded with CNFs and GNPs were investigated by a three-step dynamic heating program between − 50 °C and 300 °C considering a first run from − 50 °C up to 300 °C at 10 °C min^{-1}, a second run from 300 °C to − 50 °C at 50 °C min^{-1}, and a third run from − 50 °C up to 300 °C at 10 °C min^{-1} (Figs. 3, 4, 6, 7).

A single heating run from 0 °C up to 300 °C at 10 °C min^{-1} was used to investigate the samples oven cured at 200 °C. The DC was determined in accordance with Eq. 1 previously reported. The results of calorimetric investigation

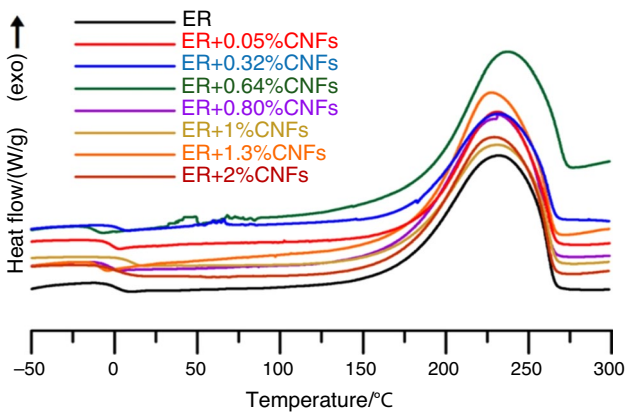

Fig. 3 DSC curves (dynamic regime) of the ER and samples loaded with different CNF mass loading percentages

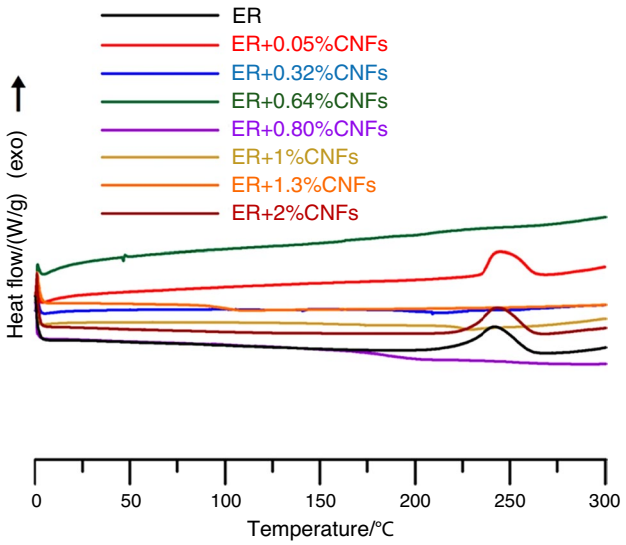

Fig. 4 DSC curves (isothermal regime) of the ER and samples loaded with different CNF mass loading percentages

carried out using both the dynamic regime and the isothermal regime are shown in Figs. 5, 8.

From Fig. 5, we can observe that all the examined samples show DC values higher than 97% also in isothermal regime. For a mass percentage of nanofiller lower than 0.025, only a slight decrease in the degree of cure is observed. The efficiency of curing process in isothermal regime is increased due to the addition of the CNFs. All the composites based

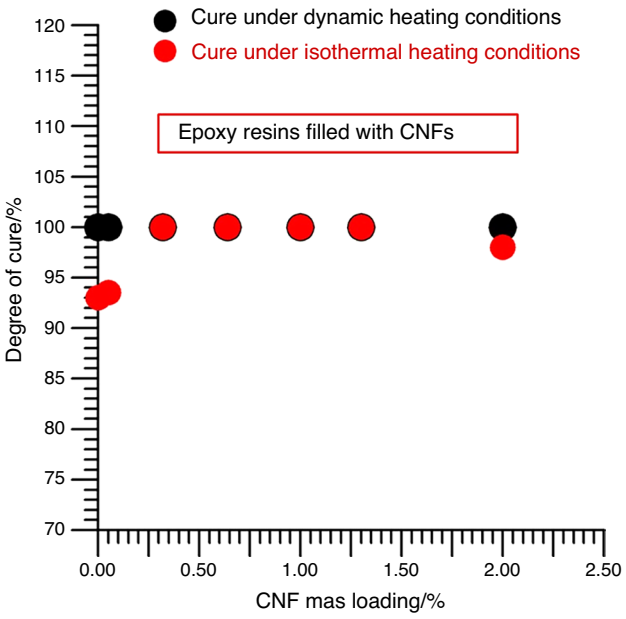

Fig. 5 Percent values of the degree of cure (DC) of the epoxy resins filled with different CNF mass loading percentages (dynamic regime and isothermal regime)

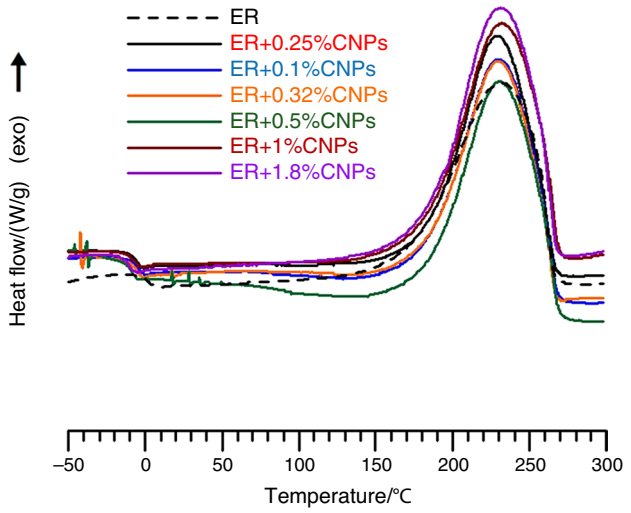

Fig. 6 DSC curves (dynamic regime) of the ER and samples loaded with different GNP mass loading percentages

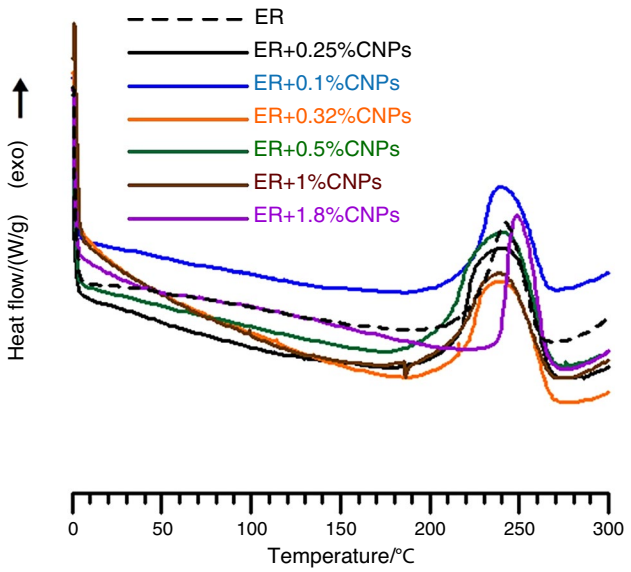

Fig. 7 DSC curves (isothermal regime) of the ER and samples loaded with different GNP mass loading percentages

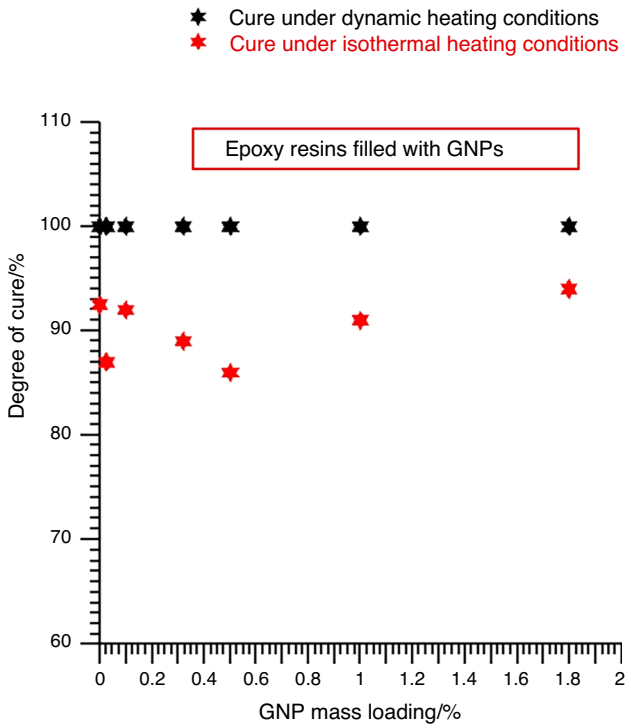

Fig. 8 Percent values of the degree of cure (DC) of the epoxy resins filled with different GNP mass loading percentages (dynamic regime and isothermal regime)

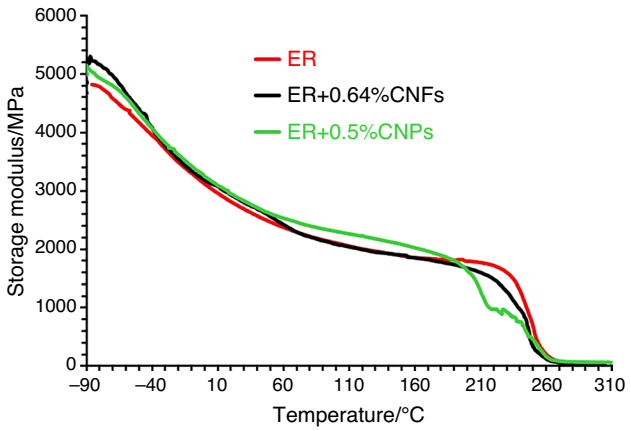

Fig. 9 Storage modulus vs. T curves of the ER, ER + 0.64%CNFs, and ER + 0.5%GNPs samples

on CNFs show a degree of cure higher than that obtained for the ER resin, even reaching a value almost of 100%. From Fig. 8, even for low mass percentages of GNPs, the DC is very close to 90%, reaching up to 95% for the sample loaded with 1.8 mass% of GNPs, thus improving the efficiency of the isothermally curing process. The results on the resins filled with CNFs and GNPs nanofillers highlight the ability of both the 1D filler and the 2D filler to act beneficially on the curing degree, fully satisfying the rigid requirements imposed by the industries operating in the field of structural functional resins, such as aeronautics and wind energy.

The profiles of the curves related to the storage modulus and loss factor (tanδ) of the three samples ER, ER + 0.64%CNFs, and ER + 0.5%GNPs are displayed in Figs. 9 and 10.

From the storage modulus curve (Fig. 9), we observe a trend that allows us to clearly identify the relaxation mechanisms due to the glass transition temperature (Tg) of the samples under investigation. For all samples, we note a rapid

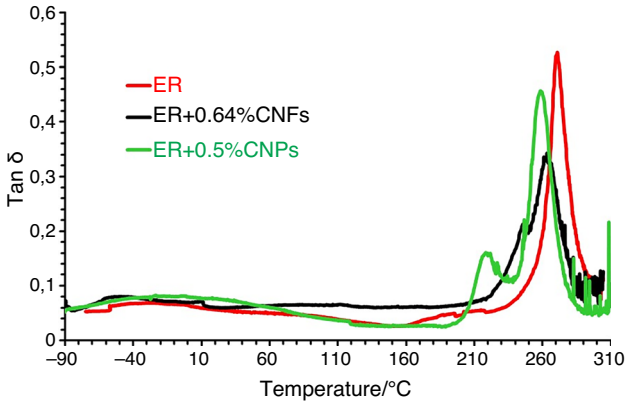

Fig. 10 Tan δ vs. T curves of the ER, ER + 0.64%CNFs, and ER + 0.5%GNPs samples

decrease by increasing the temperature in the range between − 90 °C and 60 °C. For a further increase in the temperature, we detect a less marked decrease up a very rapid drop due to the glass transition temperature. This thermal event falls within a range depending on the nature of the sample. In particular, for the unfilled sample, the drop due to the Tg is detected at slightly higher temperatures (between 240 °C and 270 °C), while for the sample filled with nanofibers the drop starts a little earlier, at the temperature of 210 °C. This drop is slightly anticipated for the sample containing graphene nanoplatelets. For this last sample, we can also observe a discontinuity in the fall that occurs through a double stage. This trend is certainly due to a further increase in cross-linking caused by the high temperatures and by the greater mobility of the chains at values of temperature around the Tg. This hypothesis is very plausible and appears to be confirmed by thermal data. In fact, the sample containing graphene nanoplatelets solidified in a static temperature regime is characterized by a degree of cure lower than 100%. It is very likely that the two stages of the fall are due to the completion of the curing.

The trend of the loss factor (tanδ) clearly evidences the behavior discussed in relation to the storage modulus. Also in Fig. 10, we can see in the green graph relaxations mechanisms at lower temperatures associated with a phase fraction characterized by higher mobility (transition at lower temperatures) diagnostic of domains with a lower curing degree. In fact, a transition around 210 °C is observed, before the main glass transition temperature detectable around 260 °C.

Figures 11-14 show the TUNA characterization of the ER + 1.3%CNFs and ER + 1.8%GNPs nanocomposites. In particular, Figs. 11 and 13 show height, deflection error and TUNA current pictures of the fracture surface of the samples ER + 1.3%CNFs and ER + 1.8%GNPs, respectively. Figures 12 and 14 show the profile of the current variations (on the right) along the three white lines drawn in the TUNA current image (on the left) of the fracture surface of the samples ER + 1.3%CNFs and ER + 1.8%GNPs, respectively.

From the TUNA images, the morphological peculiarities correlated with the type of nanofiller homogeneously dispersed in the epoxy resin and to the effectiveness of the interfacial interaction between the host matrix and the nanofiller, which results from the formation of a highly cross-linked conductive network, are distinctly detectable. The different types of TUNA images allow obtaining, through comparison, a complementarity of information not clearly deducible from a single image. The scale bar associated with each image shows a range of colors that are directly related to the colors present in the height, deflection error and TUNA current maps of the investigated samples.

We can undoubtedly observe the conductive network of CNFs and GNPs strongly anchored to the epoxy matrix, markedly visible in TUNA current images. In this regard, for the samples ER + 1.3%CNFs and ER + 1.8%GNPs, the white ellipse and the white arrows indicate the interconnected carbon nanofibers which are also intimately linked to the polymeric matrix (TUNA current picture in Fig. 11) and the graphene nanoplatelets that appear very close to each other as if to touch and homogeneously dispersed in the host matrix in which they seem to be well embedded

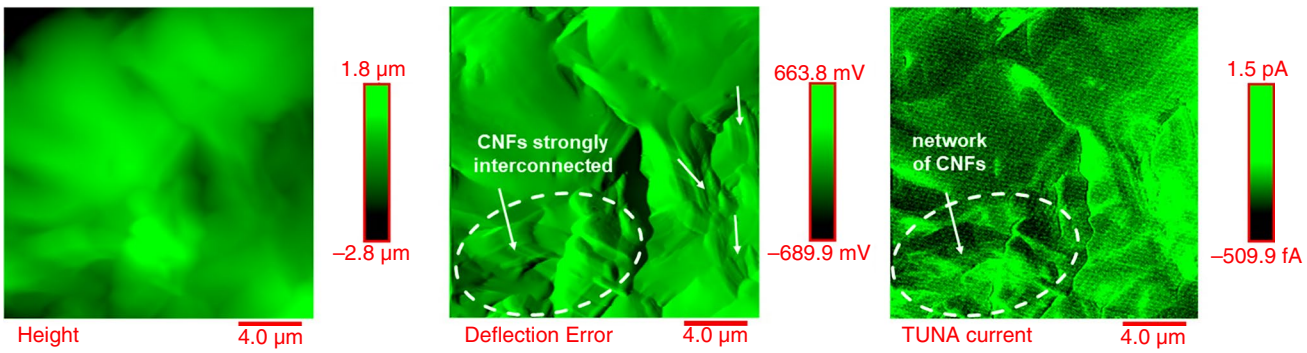

Fig. 11 TUNA pictures of the ER + 1.3%CNFs fracture surface

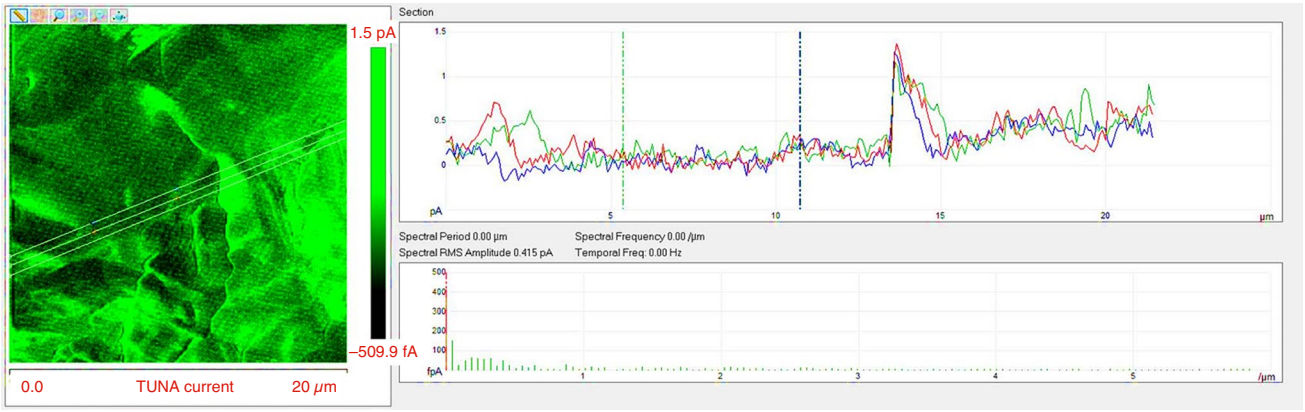

Fig. 12 Profile of the current variations (on the right) along the three white lines drawn in the TUNA current image (on the left) of the ER + 1.3%CNFs fracture surface

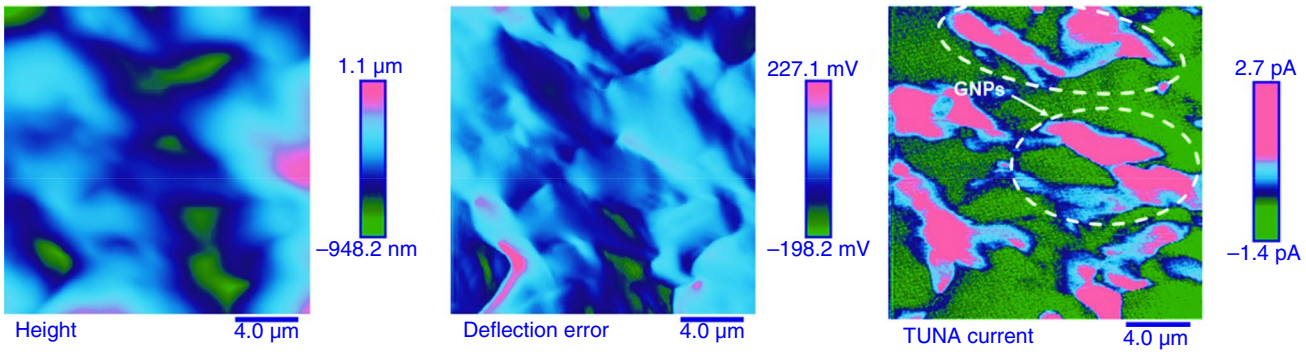

Fig. 13 TUNA pictures of the ER + 1.8%GNPs fracture surface

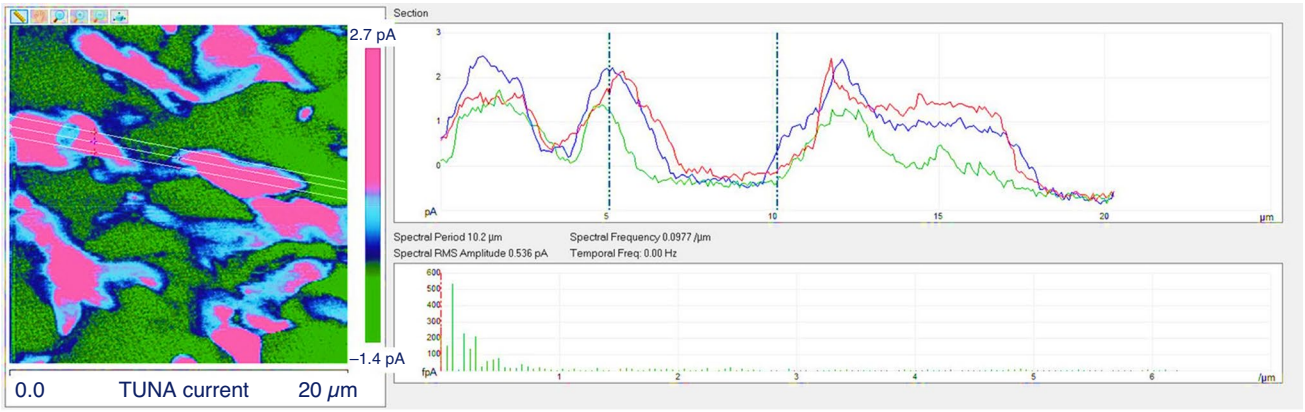

Fig. 14 Profile of the current variations (on the right) along the three white lines drawn in the TUNA current image (on the left) of the ER + 1.8%GNPs fracture surface

thanks to the strong interaction with the resin (TUNA current picture in Fig. 13). In the TUNA current images, the presence of the luminous strands of the carbon nanofibers of light green color and the graphene nanoplatelets characterized by a bright pink color on the surface and at the edges with shades of intense blue demonstrate that both the nanocomposites are intrinsically conductive. The TUNA current images show an increased contrast in the morphological features of CNFs and GNPs nanofillers. In the current profiles, domains with different brightnesses present differences

in the current value. For the sample ER + 1.3%CNFs, currents ranging from − 509.9 fA to 1.5 pA and for the sample ER + 1.8%GNPs currents ranging from − 1.4 pA to 2.7 pA were detected. The possibility to detect such low currents (ranging from fA to pA) in these nanocomposites, whose concentration is above the EPT, confirms the relatively high value of the electrical conductivities of both nanocomposites (1.37 S/m in the case of ER + 1.3%CNFs [5] and 0.096 S/m in the case of ER + 1.8%GNPs [2]) and the effective conductive paths due to a good conductive nanofiller dispersion as it is highlighted by the strong contrast of the colors in the TUNA Current micrographs.

Through the TUNA current images, we were able to evaluate the dispersion of the CNFs and GNPs within the epoxy matrix. In this regard, Figs. 12 and 14 show for the fracture surface of the samples ER + 1.3%CNFs and ER + 1.8%GNPs, respectively, TUNA current pictures where the three white lines are visible and the corresponding current variations (along the three white lines) are represented by green, red, and blue graphics on the right. We can observe that for both the samples, the frequency of the changes due to filler/matrix interchanges along the three lines is evenly constant. This unquestionably demonstrates a good distribution of both 1D and 2D nanofillers. Besides, the profiles of the current variations along the three white lines drawn in the TUNA current images (Figs. 12 and 14) that have been outlined through the section analysis are strongly representative of the electrical response localized in the nanodomains. This response is attributable to the intrinsic conductivity of the specific nanofiller as well as to the effective dispersion of the nanofiller in the host matrix and to the ability of the nanofiller to interpenetrate with matrix through the formation of a highly cross-linked conductive network.

Conclusions

In this work, samples containing dispersed carbon nanostructured forms, such as CNFs and GNPs, capable to impart electrical conductivity, have been analyzed using thermal analysis. The investigated nanocomposites manifest very high values of curing degree (almost 100% in the case of CNFs). These results are relevant in light of the modality of the performed curing cycle. In fact, they have been obtained for samples solidified in isothermal conditions. This aspect is of the utmost importance because the curing process (solidification of the nanofilled formulations) in isothermal conditions well simulates the real curing procedures adopted by manufacturers of aeronautical composites and others industrial fields. Graphene-based nanoparticles also are able to confer high DC to the same hosting matrix. In fact, even for low mass percentages of GNPs, the DC is very close to 90%, reaching up to 95% for the sample loaded with 1.8 mass% of GNPs. The calorimetric results clearly demonstrate the ability of both 1D and 2D carbon nanofillers to increase the efficiency of curing process in isothermal regime, thus giving rise to a highly cross-linked network which is also evident from the morphological TUNA characterization of the conductive nanodomains of the nanocomposites loaded with mass percentages of CNFs and GNPs beyond the EPT. The high curing degree was achieved using a suitable two-stage curing cycle and an efficacious hardener even for a low nanofiller amount. In conclusion, the winning combination of the good thermal and mechanical properties and the excellent electrical performance imparted by the chosen nanofillers make the formulated nanocomposites suitable for multifunctional application in various industrial sectors where also functional properties are required.

Authors' Contribution The authors have no conflicts of interest to declare that are relevant to the content of this article.

References

1. Benega MAG, Silva WM, Schnitzler MC, Andrade RJE, Ribeiro H. Improvements in thermal and mechanical properties of composites based on epoxy-carbon nanomaterials: a brief landscape. Polym Testing. 2021;98: 107180. https://doi.org/10.1016/j.polymertesting.2021.107180.
2. Raimondo M, Guadagno L, Speranza V, Bonnaud L, Dubois P, Lafdi K. Multifunctional graphene/POSS epoxy resin tailored for aircraft lightning strike protection. Compos Part B Eng. 2018;140:44–56. https://doi.org/10.1016/j.compositesb.2017.12.015.
3. Verma D, Gope PC, Shandilya A, Gupta A. Mechanical-thermal-electrical and morphological properties of graphene reinforced polymer composites: a review. Trans Indian Inst Met. 2014;67:803–16. https://doi.org/10.1007/s12666-014-0408-5.
4. Nobile MR, Raimondo M, Naddeo C, Guadagno L. Rheological and morphological properties of non-covalently functionalized graphene-based structural epoxy resins with intrinsic electrical conductivity and thermal stability. Nanomaterials. 2020;10(7):1310. https://doi.org/10.3390/nano10071310.
5. Raimondo M, Guadagno L, Vertuccio L, Naddeo C, Barra G, Spinelli G, Lamberti P, Tucci V, Lafdi K. Electrical conductivity of carbon nanofiber reinforced resins: potentiality of tunneling atomic force microscopy (TUNA) technique. Compos Part B Eng. 2018;143:148–60. https://doi.org/10.1016/j.compositesb.2018.02.005.
6. Raimondo M, Naddeo C, Vertuccio L, Lafdi K, Sorrentino A, Guadagno L. Carbon-based aeronautical epoxy nanocomposites: effectiveness of atomic force microscopy (AFM) in investigating the dispersion of different carbonaceous nanoparticles. Polymers. 2019;11(5):832. https://doi.org/10.3390/polym11050832.
7. Naddeo C, Guadagno L, De Luca S, Vittoria V, Camino G. Mechanical and transport properties of irradiated linear low density polyethylene (LLDPE). Polym Degrad Stab. 2001;72(2):239–47. https://doi.org/10.1016/S0141-3910(01)00025-8.
8. Naddeo C, Guadagno L, Vittoria V. Photooxidation of spherilene linear low-density polyethylene films subjected to environmental weathering 1 Changes in mechanical properties. Polym Degrad

Stab. 2004;85(3):1009–13. https://doi.org/10.1016/j.polymdegradstab.2003.04.005.
9. Guadagno L, Naddeo C, Raimondo M, Gorrasi G, Vittoria V. Effect of carbon nanotubes on the photo-oxidative durability of syndiotactic polypropylene. Polym Degrad Stab. 2010;95(9):1614–26. https://doi.org/10.1016/j.polymdegradstab.2010.05.030.
10. Guadagno L, Naddeo C, Raimondo M, Speranza V, Pantani R, Acquesta A, Carangelo A, Monetta T. UV irradiated graphene-based nanocomposites: change in the mechanical properties by local harmoniX atomic force microscopy detection. Materials. 2019;12(6):962. https://doi.org/10.3390/ma12060962.
11. Idumah CI, Hassan A. Emerging trends in graphene carbon based polymer. Rev Chem Eng. 2016;32(2):223–64. https://doi.org/10.1515/revce-2015-0038.
12. Araby S, Philips B, Meng Q, Ma J, Laoui T, Wang CH. Recent advances in carbon-based nanomaterials for flame retardant polymers and composites. Compos Part B Eng. 2021;212: 108675. https://doi.org/10.1016/j.compositesb.2021.108675.
13. Al Sheheri SZ, Al-Amshany ZM, Al Sulami QA, Tashkandi NY, Hussein MA, El-Shishtawy RM. The preparation of carbon nanofillers and their role on the performance of variable polymer nanocomposites. Des Monomers Polym. 2019;22(1):8–53. https://doi.org/10.1080/15685551.2019.1565664.
14. Loos MR, Ferreira Coelho LA, Pezzin SH, Amico SC. Effect of carbon nanotubes addition on the mechanical and thermal properties of epoxy matrices. Mater Res. 2008;11(3):347–52. https://doi.org/10.1590/S1516-14392008000300019.
15. Blanco I, Cicala G, Faro CL, Recca A. Development of a toughened DGEBS/DDS system toward improved thermal and mechanical properties by the addition of a tetrafunctional epoxy resin and a novel thermoplastic. J Appl Polym Sci. 2003;89(1):268–73. https://doi.org/10.1002/app.12179.
16. Blanco I, Cicala G, Faro CL, Motta O, Recca G. Thermomechanical and morphological properties of epoxy resins modified with functionalized hyperbranched polyester. Polym Eng Sci. 2006;46(11):1502–11. https://doi.org/10.1002/pen.20604.
17. Blanco I, Cicala G, Motta O, Recca A. Influence of a selected hardener on the phase separation in epoxy/thermoplastic polymer blends. J Appl Polym Sci. 2004;94(1):361–71. https://doi.org/10.1002/app.20927.
18. Zhou YX, Pervin F, Lewis L, Jeelani S. Experimental study on the thermal properties of multi-walled carbon nanotube reinforced epoxy. Mater Sci Eng A. 2007;452:657–64. https://doi.org/10.1016/j.msea.2006.11.066.
19. Guadagno L, Raimondo M, Vittoria V, Vertuccio L, Naddeo C, Russo S, De Vivo B, Lamberti P, Spinelli G, Tucci V. Development of epoxy mixtures for application in aeronautics and aerospace. RSC Adv. 2014;4:15474–88. https://doi.org/10.1039/C3RA48031C.
20. Binder K, Gennes PG, Giannelis EP, Grest GS, Hervet H, Krishnamoorti R, Léger L, Manias E, Raphaël E, Wang SQ. Polymers in confined environments. 1st ed. Berlin: Springer; 1999.
21. Bhat A, Budholiya S, Raj SA, Sultan MTH, Hui D, Md Shah AU, Safri SNA. Review on nanocomposites based on aerospace applications. Nanotechnol Rev. 2021;10:237–53. https://doi.org/10.1515/ntrev-2021-0018.
22. Kleiman JI, Tagawa M, Kimoto Y, editors. Protection of materials and structures from the space environment. Berlin: Springer; 2006.
23. Bannov AG, Popov MV, Kurmashov PB. Thermal analysis of carbon nanomaterials: advantages and problems of interpretation. J Therm Anal Calorim. 2020;142:349–70. https://doi.org/10.1007/s10973-020-09647-2.
24. Guadagno L, Raimondo M, Vertuccio L, Mauro M, Guerra G, Lafdi L, De Vivo B, Lamberti P, Spinelli G, Tucci V. Optimization of graphene-based materials outperforming host epoxy matrices. RSC Adv. 2015;5:36969–78. https://doi.org/10.1039/c5ra04558d.
25. Chung DDL. A review of exfoliated graphite. J Mater Sci. 2016;51(1):554–68. https://doi.org/10.1007/s10853-015-9284-6.
26. Nobile MR, Raimondo M, Lafdi K, Fierro A, Rosolia S, Guadagno L. Relationships between nanofiller morphology and viscoelastic properties in CNF/epoxy resins. Polym Compos. 2015;36(6):1152–60. https://doi.org/10.1002/pc.23362.